A SERS-Active System Based on Silver Nanoparticles Tethered to a Deposited Silver Film

D. J. Anderson

Department of Chemistry University of Toronto, Toronto, Ontario, Canada M5S 3H6

M. Moskovits*

Department of Chemistry and Biochemistry, University of California, Santa Barbara, California 93106

Received: September 15, 2005; In Final Form: April 22, 2006

A series of SERS-active nanostructures were produced by exposing a freshly deposited silver film (fabricated to be as free from roughness as practicable) to a solution containing a mixture of 1-decanethiol (**m**) and 1,9-nonanedithiol (**d**) of varying concentrations of **m** to **d**, then allowing colloidal silver nanoparticles to interact with the surface. Silver nanoparticles were found to bind exclusively to films which were prepared from solutions with a nonzero concentration of the dithiol implying that the nanoparticles were tethered to the silver surface by the dithiol with one of the thiolate groups bound to the nanoparticle and the other to the silver film. Intense SERS spectra were observed even from samples in which the **m**/**d** concentration ratio was so large that the adsorbed molecules in the vicinity of only $\sim 8 \pm 3$ nanoparticles were illuminated by the diffraction-limited focused laser beam. At such high dilution, the molecules (numbering at most ~330) residing in the SERS "hot spots" associated with the ~8 nanoparticles consisted primarily of **m** (although, of course, for each nanoparticle, at least one molecule in the hot spot had to be **d** to serve as the linker). This was corroborated by the SERS spectra. An analysis is presented, which accounts for the fact that as the concentration ratio of **m**/**d** increases, the SERS intensity associated with bands belonging to **m** first increases to a maximum then decreases. The nanoparticle−metal film system presented here is a simple embodiment of a more general range of SERS-active sensing platforms in which a molecular tether is used to create a SERS hot spot that (although nanosized) is large enough to accommodate analyte molecules that cannot themselves function as linkers, which are subsequently detected by SERS at the few-molecule level.

Introduction

Surface enhanced Raman spectroscopy (SERS) is a phenomenon associated with the intensification of the incident and Raman-scattered optical fields arising from the excitation of localized surface plasmons in appropriately nanostructured metal, among which the most effective are silver and the alkali metals followed by gold and copper.[1] This enhancement mechanism is referred to as electromagnetic (em) enhancement.[2] In addition to the em effect, a variety of other resonances contribute to the SERS intensity. These are collectively referred to as chemical enhancement.[3] It has long been recognized that the most effective SERS-active systems consist of assemblies of strongly interacting nanoparticles[4,5] and, when these assemblies are nanoparticle dimers or small clusters,[4] the most effective locations for enhancement are interstitial sites, hot spots, between particles. In such systems the enhancement intensity depends critically on the interparticle distances, the polarization, and the wavelength of the exciting light. The wavelength at which enhancement is greatest will depend on the cluster geometry and the interparticle distances. Local SERS enhancements exceeding $\sim 10^{11}$ are possible in such systems. Recent calculations[6] and experimental results[7] suggest that at favored locations within aggregates of core−shell particles (e.g., a dielectric core surrounded by a silver or gold shell) even greater enhancements are possible, perhaps exceeding 10^{13}. Renewed interest in SERS enhancement by small nanoparticle clusters and other nanostructured systems followed the realization that single-molecule SERS[8] arose from the excitation of molecules located in the hot spots of such systems.[9]

Although one can conceive of important applications for dimers and small aggregates as SERS substrates, they are not ideal SERS substrates for a number of reasons. First, as previously stated, the resonance conditions will be cluster-geometry-dependent obligating the user to produce clusters of known and reproducible geometries (a challenging task). Second, the molecules whose SERS spectrum is desired must be located reproducibly at a specific "hot spot" in the cluster. Finally, the system needs to be designed so that a cluster is easily found. One way to ensure a broad resonance condition thereby avoiding the first problem is to create large, fractal nanoparticle aggregates which have been shown to have intense resonances over a very broad wavelength range.[5] However, while the hot spots associated with these resonances are localized, the positions of these hot spots within the aggregate are not predictable without precise knowledge of the location of every particle in the fractal aggregate, leaving the second and third of the above limitations unmet.

One SERS platform that meets some of these requirements with properties consistent with the goal of reliability, reproducibility, and applicability to a broad range of molecular analytes consists of a uniform (but not periodic) layer of silver nanoparticles tethered to a silver film covering a large enough area to make every location on the film, on average, more or less identical (Figure 1). When illuminated with laser light, this

* To whom correspondence should be addressed. E-mail: mmoskovits@LTSC.ucsb.edu.

10.1021/jp055243y CCC: $33.50
Published on Web 06/23/2006

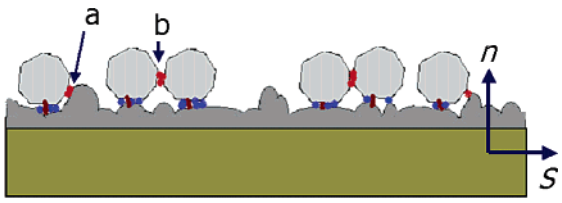

Figure 1. Schematic of a silver nanoparticle (light gray) array tethered to a silver film (dark gray) deposited on an appropriate substrate (tan) using an appropriate tethering linker such as an $\alpha\omega$ dithiol or diamine (dark brown). This creates a number of hot spots below the nanoparticles (blue) that are most active when the system is illuminated with light polarized normal (*n*) to the average surface of the substrate, between neighboring nanoparticles (b-sites) that can be excited by light polarized along the average substrate surface (*s*), or between nanoparticles and vicinal surface asperities (a-sites) (red). The a-sites can, depending on the local geometry of the particle-asperity gap, contribute significantly either when *n* or *s* polarization is used. Either or both the nanoparticles and the underlying silver film can be appropriately (and completely) functionalized with a molecular-recognition agent so as to restrict subsequent bonding to the SERS-active system to analyte molecules that bind to the molecular recognition agent, thereby improving the rather-unspecific affinity of silver (or gold).

arrangement is approximately equivalent to an ensemble of nanoparticle dimers or clusters, because the field distribution near the surface of such a system arising from the combined effect of the incident field plus the field resulting from the charge dynamics in the nanoparticles is approximately equivalent to those between the nanoparticles and charge-conjugate images of the nanoparticles in the silver. (Because silver is not an ideal conductor, the image charges do not perfectly reflect the charges in the nanoparticle, but the equivalence is quite good and can therefore serve as a conceptual aid in designing SERS-active systems.) This fact was already recognized over two decades ago[10]. In designing such a nanoparticle−metal film system, one can also take advantage of the additional enhancement expected from core−shell particles by tethering silver-coated silica nanoparticles, for example, to a solid silver layer. The image particles will mimic a charge-conjugate core−shell particle. Because atomically smooth films are difficult to fabricate, the system shown in Figure 1 also shows some enhancement from the coupling of the tethered nanoparticles to surface asperities.

Referring to Figure 1, the benefits and remaining limitations of this approach are as follows. First, by using a tethering linker of uniform length one produces a system with a somewhat tighter distribution of particle-to-surface distances. Creating a random rather than a periodic distribution of particles will also broaden the resonance condition (although not as much as for a fractal particle aggregate[5]), making near-reproducible performance film-to-film possible for a given excitation wavelength. The system will display two types of hot spots. The first is those between particles and the surface underneath those particles. Such hot spots will be effective primarily for light polarized normal to the surface (designated as *n* in Figure 1), although for interacting assemblies of tethered particles, and at some wavelengths this polarization condition can be relaxed. The second general type of hot spot (designated b-sites in Figure 1) is situated between neighboring nanoparticles. These, in general, will be active for light polarized parallel to the surface of the substrate (designated as *s* in Figure 1). For generality we must include hot spots formed between nanoparticles and surface asperities (a-sites in Figure 1), which, could be excited with light of one or both of the above-mentioned polarizations, depending on the local geometry of that site.

In the most powerful embodiment of this approach, the surface would be functionalized so that it becomes most sensitive to a particular analyte or a particular class of analytes, by preadsorbing a molecular species along with the linkers that act as molecular recognition agents toward the desired analyte. An effective approach would be to use rather few linkers among very many molecules that function as molecular recognition agents toward the analyte, so that in the majority of cases the silver (or gold) nanoparticle is tethered to the surface by a single linker, while the hot spot created in the neighborhood of the nanoparticle accommodates several analyte molecules. The SERS spectrum would then be dominated by that of the analyte. Moreover, the dominance of the spectrum by the analyte can be made more striking by choosing a linker with a simple molecular structure (such as an alkyl dithol or diamine) whose spectrum is consequently uncluttered.

Limitations remain, however, including poor control over particle-to-particle distances and imperfect control on the structure of the underlying film. These might be ameliorated somewhat through various refinements, such as creating linked rafts of nanoparticles that are then deposited and tethered to the silver surface.[11]

In this paper we illustrate the approach by producing a system approximating that illustrated in Figure 1. Specifically, colloidal silver nanoparticles are linked to a freshly deposited silver film via a dithiol linker diluted with a monothiol that serves the role of the analyte. The surface density of silver nanoparticles is varied by exposing the deposited silver film to mixtures of a 1,9-nonanedithiol (**d**) and 1-decanethiol (**m**) of various ratios. The lone thiol group of **m** binds to the surface of the silver film thereby simultaneously playing the role of the analyte and passivating the silver film toward subsequent binding of the silver nanoparticles (as well as toward the adsorption of undesirable species from the environment). In choosing an appropriate linker, such as a dithiol, one must guard against the propensity for both thiolated ends to bind to the silver film, which can be accomplished by choosing either a short enough or a stiff enough linker while retaining the other terminal thiol as a possible binding site for the silver nanoparticles.

Experimental

Silver sols were produced as previously described.[12] Briefly, a 2.0 mM solution of sodium borohydride ($NaBH_4$, Aldrich, used as received) was prepared and cooled to 4 °C in an ice bath. A solution of 1.0 mM silver nitrate ($AgNO_3$, Aldrich, used as received) was prepared and added dropwise in a 1:3 v/v ratio to the $NaBH_4$ solution while stirring continuously. If visible aggregation occurred (indicated by the presence of black or brown clouds in solution) the addition of $AgNO_3$ was halted, and the solution was stirred until the aggregation stopped. When $AgNO_3$ addition was complete, stirring was continued for an hour, and the solution was stored in the dark and in brown glass bottles as a precaution against photoaggregation. The nanoparticles so produced have a mean diameter of ∼20 nm.

Ag films were vapor-deposited in a vacuum on precleaned glass substrates, with the use of a tungsten wire boat holding silver pellets (5 N, Alfa Aesar). Prior to deposition, the vacuum chamber was evacuated to 10^{-7} Torr for 30 min to 1 h. The tungsten boat was first resistively heated for ∼30 min to a temperature below which silver evaporation occurred, to outgas the metal deposition system and the chamber. The current was then increased until a deposition rate of approximately 0.1 nm/min was achieved. Silver layers with a thickness of ∼100 nm were prepared, as measured by a piezoelectric thickness monitor. If not used immediately after deposition, samples were placed into a desiccator under nitrogen and stored in the dark. A film-

TABLE 1: Key to the (C_m/C_d) Ratios

series	(C_m/C_d)	obsd no. of nanoparticles per μm^2	N_{Ag}, calcd no. of nanoparticles per μm^2 (see discussion)
A	0 (pure **d**)	125 ± 20	125 (assumed)
B	0.04		
C	20	75 ± 20	123
D	2000	8 ± 3	6
E	200 000	0	.06
F	∞ (pure **m**)	0	

deposition protocol was used that would produce films that had as little roughness as possible, that is, films that are not good SERS substrates in themselves, so as to maximize the SERS enhancement effect of the tethered nanoparticles.

For experiments involving single-component solutions of 1-decanethiol and 1,9-nonanedithiol, 1.0 and 0.10 mM ethanol solutions were used. For the mixed **m** + **d** experiments, a 1 mM solution of **m** was mixed with an appropriately diluted solution of **d** to yield the desired ratio. The freshly produced silver substrate was exposed to the thiol solution for 30 min and was then rinsed repeatedly with absolute ethanol to wash off physisorbed molecules. The substrate was then placed into the colloidal silver solution for 30 min. After removal from solution, the substrate was washed in absolute ethanol and distilled water and was stored under nitrogen in a desiccator until used for the SERS or SEM measurements. (Glassware was rinsed in acetone, then immersed for 12−24 h in concentrated nitric acid and, post-immersion, rinsed in acetone followed by repeated rinsing with distilled water.)

Raman spectra were recorded using a backscattering configuration on a JobinYvon LabRam microRaman system equipped with a confocal microscope. Spectra were excited by 0.4 mW of 514.5 nm Ar ion laser radiation. The laser beam was focused to a diffraction-limited spot with area < 1 μm^2. Collection times were 30 s.

High-resolution scanning electron microscope images were collected using a Hitachi S-4500 FE-SEM, Field-Emission SEM.

Results and Discussion

Six series of experiments were carried out in which the monothiol-to-dithiol ratio, C_m/C_d, was varied. The series labeled A through F correspond to the C_m/C_d values shown in Table 1, which also lists the average number of nanoparticles observed by SEM per μm^2. Two typical SEM images are shown in Figure 2. Figure 3 shows a series of SERS spectra measured for the six sample types with the laser beam normal to the substrate surface (corresponding to the incident electric vector parallel to the surface, i.e., *s*-polarization).

The spectra shown in Figure 3 indicate that even in the absence of added nanoparticles the silver films are sufficiently rough to show very weak SERS signals. The SERS intensity increased significantly on linking silver nanoparticles to the surface, provided that several nanoparticles resided in the focal spot of the focused laser beam.

The assignments of the observed Raman bands are summarized in Table 2. For series E the average number of nanoparticles per μm^2 was significantly smaller than unity. As a result, the SERS spectrum recorded for the E samples differed only very little from those of the F (no dithiol) samples. In both cases, essentially no surface-bound nanoparticles could be found in the SEM images. The SEM results indicate that, on average, the spectra reported for the D samples originate from ~8 ± 3 nanoparticles. On the basis of an estimate of the molecular area occupied by a single adsorbed **m** and assuming that the hot spot occupies a circular area with a diameter equal to the average radius of the nanoparticle, we estimate that ~30 molecules can be accommodated in the hot spot. Accordingly, spectrum D is due to at most ~330 molecules.

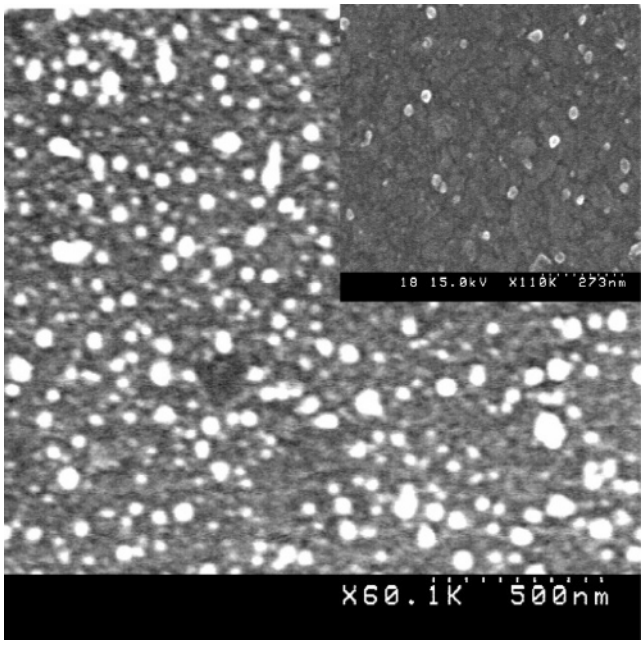

Figure 2. Two SEM micrographs of silver nanoparticles linked to a silver film using dithiol linkers. The large figure was obtained when only dithiol was adsorbed onto the silver surface. The inset corresponds to the specimen produced when silver nanoparticles were allowed to come into contact with a film on which a mixture of thiol and dithiol was adsorbed out of a solution in which the thiol to dithiol concentration ratio was 20.

The SERS spectra for series E and F show only very weak Raman bands. Other than the broad feature at ~1550 cm^{-1} which we attribute to mesoscopic, disordered graphitic carbon, a ubiquitous species with a large Raman cross-section in SERS spectra,[15] only very weak bands associated with the C−S stretching vibration are observed.

By contrast, spectra A through D show other intense SERS bands in addition to the 1550 cm^{-1} graphitic band, which nevertheless dominates spectra A through C. This graphitic feature is also present in spectrum D but does not dominate. The most prominent and noteworthy spectroscopic observations and trends are the strong bands observed at 640 and 698 cm^{-1} in spectra A through F. These are almost certainly the C−S stretching vibration, $\nu(C-S)_G$ and $\nu(C-S)_T$, respectively, corresponding to molecules with gauche and trans conformations.[13] The presence of these bands also indicates that **m** and **d** adsorb as the thiolate. The trans mode increases a little in relative intensity with respect to the lower frequency mode as the **m**/**d** ratio increased (i.e., as one proceeds from samples A to E). The high intensity of these modes is understandable in view of their proximity to the silver surface, assuming the thiols bind to the silver through the sulfur. The weak vestiges of these bands observed in spectrum F are more than 30 times weaker than those observed in spectrum A, implying that although the Ag films possess residual roughness so that the bands with large SERS cross sections such as the C−S and the graphitic bands are weakly visible even in the absence of tethered nanoparticles, it is fair to say that the Ag films themselves (at least as produced for this study) are poor SERS substrates, whereas the films with tethered nanoparticles are excellent SERS substrates, so that molecular species present in the hot spots created by tethering

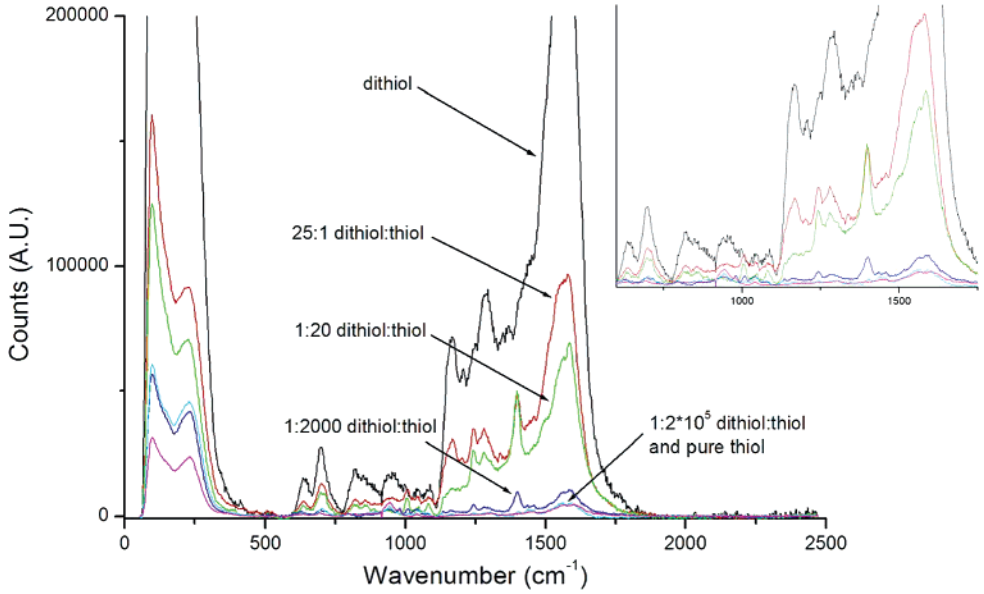

Figure 3. SERS spectra recorded for a series of silver films to which silver nanoparticles were linked using a dithiol linker. Spectra are labeled to indicate various ratios of thiol to dithiol concentration in the solution out of which these molecules were adsorbed onto the silver films.

TABLE 2: Observed SERS Bands and Assignements

obsd SERS band frequency/cm^{-1}	literature value[a]	assignt	notes
1550		graphitic carbon	
1400	1380	CH_3 sym def	not obsd in A
1294	1301	CH_2 wag	
1246		unassigned	
1205		unassigned	obsd only in A
1172	1123	$\nu_s(C-C)_T$	
1087	1062	$\nu_a(C-C)_T$	
1039	1029	$\nu(C-C)_{T/G}$	
941		unassigned	
824	862	CH_2 (rock)$_G$	
698	704	$\nu(C-S)_T$	
640	634	$\nu(C-S)_G$	
228	200−235	ν(Ag−S)	

[a] All but the bands observed at 228 and ~1550 cm^{-1} are compared to values reported by Sandhyarani and Pradeep.[13] The 228 is assigned by analogy to what is reported by Bensebaa et al.,[14] whereas the 1550 cm^{-1} band is likely due to mesoscopic graphitic carbon[15] which is often seen in the SERS spectra of organic molecules resulting from the decomposition (and likely photodecomposition) of the adsorbate.

nanoparticles to the silver surface would dominate the SERS spectrum, should this approach be used as an molecular analysis platform.

Another interesting trend across the series A through E is the appearance of a SERS band at ~1400 cm^{-1} when **m** is added to the adsorbate mix. This band, which is assigned to a CH_3 symmetric deformation mode, is totally absent in the spectrum of A (i.e., when the adsorbate consists of pure **d**), as it should be since the dithiol possesses no methyl groups. In fact the 1400 cm^{-1} band is the only band that can be uniquely attributable to **m**. For all other bands the overlap between features belonging to **m** and **d** is too great to distinguish the two species with confidence. The 1400 cm^{-1} band, which is clearly observable in spectrum B, grows to a maximum intensity in spectrum C, then decreases on going to D and E. This trend is easily understood. As the C_m/C_d ratio increases to a large value, most of the molecules in a hot spot (everywhere for that matter) will be **m**. However, for each nanoparticle contributing to the SERS intensity, there must exist at least one dithiol linking the nanoparticle to the surface. Hence, the number of nanoparticles illuminated by the laser beam will decrease as the C_m/C_d ratio increases, offsetting the SERS signal increase brought about by the increase in the average number of **m** in the hot spot belonging to a given nanoparticle.

We estimated above that on average ~30 molecules reside in a hot spot. Hence, in all cases with the exception of series A and B, one expects the SERS spectrum to be dominated by the spectrum of **m**. This is, in fact, observed, and the contribution of **d** to the overall SERS spectrum decreases rapidly on going from A to C. The absence of nanoparticles in the SEM images recorded for samples E and F supports the assumption that nanoparticles only bind to the silver film when sufficient dithiol is present.

The uniqueness of the 1400 cm^{-1} SERS band, the only band belonging uniquely to **m**, allows us to carry out a more robust and instructive analysis of its intensity as a function of C_m/C_d. We assume that for a SERS band to be visible, the molecule giving rise to that band must reside within a hot spot associated with one or more of the silver nanoparticles[4,6,10] bound to the surface via the 1,9-nonanedithiol linker. The surface coverages of adsorbed **m** or **d** depend on their respective concentrations (C_m and C_d) in the solution from which they adsorb according to an appropriate isotherm. (In general, the adsorption properties of the two species need not be equivalent.)

We first show that the surface concentration ratio of **m** to **d** is proportional to their concentration ratio in solution, at least when their individual adsorption behavior is governed by the Langmuir isotherm. That is, we show that

$$\frac{N_m}{N_d} = K\frac{C_m}{C_d} \tag{1}$$

The proof is straightforward. If we assume Langmuir kinetics, the equations describing the time-rates of adsorption of the **m** and **d** are

$$\frac{dN_m}{dt} = k_m C_m(S - N_m - N_d) - k_{-m}N_m \tag{2}$$

$$\frac{dN_d}{dt} = k_d C_d(S - N_d - N_m) - k_{-d}N_d \tag{3}$$

where S is the total number of surface sites available, N_m and

N_d are the respective surface coverages, and $k_{m,d,-m,-d}$ are the appropriate adsorption and desorption rate constants. The term $(S - N_m - N_d)$ equals the number of surface sites available to further adsorption. (The assumption is made that **m** and **d** occupy more or less the same molecular surface area.)

At steady state, the rates given by eqs 2 and 3 are zero. Substituting for $(S - N_m - N_d)$ from 2 into 3, produces eq 1 directly if one defines K as $k_m k_{-d}/(k_{-m} k_d)$.

We now assume that the total concentration of **m** plus **d** is constant, and that it is large enough that we have surface saturation in all of the experiments that were carried out. (This assumption is not strictly required in systems governed approximately by the same isotherm, as is assumed here.) We also assume that each nanoparticle that is attached to the surface through one or more dithiol linker (we assume one dithiol is sufficiently strong to link a silver nanoparticle to the silver surface) creates a hot spot that can accommodate more or less the same number of molecules, and that at most L nanoparticles (and their enhancing environments) can reside within the diffraction-limited laser spot illuminating the surface. We further assume that there are precisely n_T molecules that are enhanced by each of the nanoparticles and that $n_T = n_m + n_d$, where n_m and n_d are, respectively, the average number of **m** and **d** residing in a hot spot. (There are several other simplifying assumptions implicit in this analysis. For example, it is assumed that all of the molecules in a hot spot are equally enhanced. This is clearly not the case, but nor is it a damaging assumption since there will exist some (coverage-dependent) average enhancement that could replace the actual molecule-by-molecule enhancement.)

The average number of nanoparticles, $N_{Ag} \leq L$, that reside within the laser spot will be given by the probability that there exists at least one **d** within the hot spot. This probability is the complement to the probability that all of the molecules in the hot spot are **m**. The latter is given by $p_m = (n_m/n_T)^{n_T}$. Hence, the number of nanoparticles residing within the laser focus is

$$N_{Ag} = L[1 - (n_m/n_T)^{n_T}] \tag{4}$$

Because, on average, the ratio n_m/n_d is equal to the ratio N_m/N_d, which, in turn, depends on the concentration ratio, C_m/C_d, as given by eq 1 and noting that $n_T = n_m + n_d$, the following expression for n_m is obtained:

$$n_m = \frac{K n_T (C_m/C_d)}{(1 + K(C_m/C_d))} \tag{5}$$

Equation 5 plus the condition $n_T = n_m + n_d$ provide functional relations between n_m and n_d, the number of **m** and **d** molecules occupying a hot spot, and their concentration in the solution from which they were deposited. The SERS spectrum will therefore be a superposition of the spectra of the two species with relative intensities determined by the relative populations of the two species, each multiplied by the appropriate Raman cross-section.

The SERS intensity of a band that is due entirely to **m**, such as the CH_3 symmetric deformation mode, will be approximately proportional to the product of the number of monothiol molecules, n_m, in a hot spot (which we assume is associated with a single nanoparticle) and the number of active nanoparticles, N_{Ag}, illuminated by the laser beam (eq 4). That expression (as a function of $\log(C_m/C_d)$) is illustrated in Figure 4 using the assumption that $n_T = 30$ molecules and $K = 0.3$. These parameter values were chosen because they place the maximum in the SERS intensity of the 1400 cm^{-1} band at approximately the C_m/C_d ratio where the maximum is observed experimentally and simultaneously return values of N_{Ag} as a function of C_m/C_d (assuming $L = 125$) that agree, within tolerable error, with what is observed by SEM (Table 1). A value of K of 0.3 implies that **m** is only a little less likely than **d** to bind to the surface, all things being equal. Because of the simplicity of the model, no attempt was made to fit the experimentally observed data to the function $n_m N_{Ag}$ by adjusting the values of the parameters K and n_T (and a proportionality factor) using a least-squares procedure.

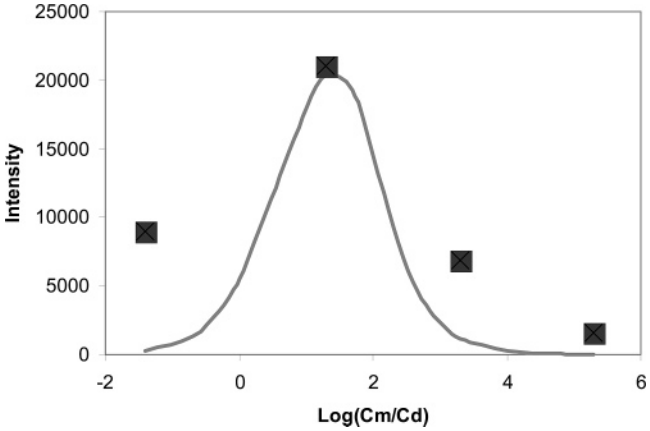

Figure 4. The SERS intensity of the CH_3 symmetric deformation mode of the 1-decanethiol as a function of the concentration ratio of the thiol to the dithiol (points). The measured values are compared to predictions of a simple model that assumes that, on average, n_T molecules (of which n_m are monothiol) will occupy the hot spot associated with a single nanoparticle. The SERS intensity is then assumed to be proportional to the product $n_m N_{Ag}$, were N_{Ag} is the number of silver nanoparticles illuminated by the laser beam. Both quantities are functions of the concentration ratio of thiol to dithiol in the solution from which these species are deposited.

In Figure 4, the measured values scaled to bring them within range of the calculated values are shown as points. Taking into account the simplicity of the model together with the fact that we are plotting values over almost 6 orders of magnitude in C_m/C_d, we find the accordance between the model and the measurements to be reasonably good.

Conclusions

Intense SERS signals were obtained from a system of silver nanoparticles tethered to a vapor-deposited silver film by 1,9-nonanedithiol (**d**). The intense SERS signal are attributed to electromagnetic "hot spots" associated with the tethered silver nanoparticles. By co-depositing 1-decanethiol (**m**) along with **d** from solutions in which the relative concentrations of **m** and **d** varied, one could produce systems of nanoparticles in which the relative *surface* concentration in a given hot spot also varied. An analysis was carried out which produced mathematical expressions for the numbers of **m** and **d** in a hot spot as a function of the ratio of the concentrations of these species in the solution from which they were deposited. The observed **m**/**d** ratio is shown to agree qualitatively with these expressions. The nanoparticle−metal film system presented here is a simple embodiment of a more general range of SERS-active sensing platforms in which a molecular tether is used to create a SERS hot spot that (although nanosized) is large enough to accommodate analyte molecules that cannot themselves function as linkers, which are subsequently detected by SERS at the few-molecule level.

Acknowledgment. This work was supported by the Natural Science and Engineering Research Council of Canada (Research Grant program) and the Canadian Institute for Advanced Research. Funding from the Institute for Collaborative Biotechnologies through Grant DAAD19-03-D- 0004 from the U.S. Army Research Office and from Lawrence Livermore National Laboratories through a UCDRD grant is gratefully acknowledged. D. J. Anderson would like to thank NSERC for an NSERC USRA fellowship that partially supported this work.

References and Notes

(1) (a) Fleischman, M.; Hendra, P. J.; McQuillan, A. J. *Chem. Phys. Lett.* **1974**, *26*, 123. (b) Jeanmaire, D. L.; Duyne, R. P. V. *J. Electroanal. Chem.* **1977**, *84*, 1. (c) Albrecht, M. G.; Creighton, J. A. *J. Am. Chem. Soc.* **1977**, *99*, 5215. (d) Otto, A. in *Light Scattering in Solids IV*; Cardona, M., Guntherodt, G., Eds.; Springer-Verlag: New York, 1984; p 289. (e) Moskovits, M. *Rev. Mod. Phys*. **1985**, *57*, 783. (f) Moskovits, M. *J. Raman Spectrosc.* **2005**, *36*, 485−496.

(2) (a) Moskovits, M. *J. Chem. Phys*. **1978**, *69*, 4l59. (b) Kerker, M.; Wang, D. S.; Chew, H. *Appl. Opt.* **1980**, *19*, 4159.

(3) (a) Otto, A.; Mrozek, I.; Grabhorn, H.; Akemann, W. *J. Phys.: Condens. Matter* **1992**, *4*, 1143. (b) Persson, B. N. *Chem. Phys. Lett*. **1981**, *82*, 561 and ref 1d.

(4) (a) Aravind, P. K.; Nitzan, A.; Metiu, H. *Surf. Sci.* **1981**, *110*, 189−128. (b) Liver, N.; Nitzan, A.; Gersten, J. I. *Chem. Phys. Lett.* **1984**, *111*, 449. (c) Wirgin, A.; López-Ríos, T. *Opt. Commun*. **1984**, *48*, 416. (d) Garcia, N.; Diaz, G.; Saenz, J. J.; Ocal, C. *Surf. Sci*. **1984,** *143*, 342. (e) Kneipp, P. A.; Reinecke, T. L.; *Phys. Rev. B: Condens. Matter Mater. Phys.* **1992**, *45*, 9091. (f) García-Vidal, F. J.; Pendry, J. B. *Phys. Rev. Lett.* **1996**, *L77*, 1163. (g) Xu H.; Käll, M. *ChemPhysChem* **2003**, *4*, 1001. (h) Li, K.; Stockman, M. I.; Bergman, D. J. *Phys. Rev. Lett.* **2003**, *91*, 227402.

(5) (a) Stockman, M. I. *Phys. Rev. E: Stat. Phys., Plasmas, Fluids, Relat. Interdiscip. Top.* **1997**, *56*, 6494. (b) Shalaev, V. M.; Botet, R.; Mercer, J.; Stechel, E. B. *Phys. Rev. B: Condens. Matter Mater. Phys.* **1996**, *54*, 8235. (c) Shalaev, V. M.; Sarychev, A. K. *Phys. Rev. B: Condens. Matter Mater. Phys.* **1998**, *57*, 13265. (d) Gresillon, S.; Aigouy, L.; Boccara, A. C.; Rivoal, J. C.; Quelin, X.; Desmarest, C.; Gadenne, P.; Shubin, V. A.; Sarychev, A. K.; Shalaev, V. M. *Phys. Rev. Lett*. **1999**, *82*, 4520. (e) Shalaev V. M. *Topics Appl. Phys*. **2002**, *82*, 113−147. (f) Markel, V. A.; Shalaev, V. M.; Zhang, P.; Huynh, W.; Tay, L.; Haslett, T. L.; Moskovits, M. *Phys. Rev. B* **1999**, *59*, 10903. (g) Drachev, V. P.; Perminov, S. V.; Rautian, S. G.; Saponov, V. P. in *Optical Properties of Nanostructured Random Media*; Shalaev, V. M. *Top. Appl. Phys*. **2002**, *82*, 113−147.

(6) (a) Talley, C. E.; Jackson, J. B.; Oubre, C.; Grady, N. K.; Hollars, C. W.; Lane, S. M.; Huser, T. R.; Nordlander, P.; Halas, N. J. *Nanoletters* **2005**, *5*, 1569−1574. (b) Oubre, C.; Nordlander, P. *J. Phys. Chem. B* **2005**, *109*, 10042−10051. (c) Oldenburg, S. J.; Averitt, R. D.; Westcott, S. L.; Halas, N. J. *Chem. Phys. Lett.* **1998**, *288*, 243−247. (d) Jackson, J. B.; Halas, N. J. *J. Phys. Chem. B* **2001**, *105*, 2743−2746. (e) Oldenburg, S. J.; Jackson, J. B.; Westcott, S. L.; Halas, N. J. *Appl. Phys. Lett.* **1999**, *111*, 2897−2899. (f) Prodan, E.; Radloff, C.; Halas, N. J.; Nordlander, P. *Science* **2003**, *302*, 419−422.

(7) (a) Jackson, J. B.; Westcott, S. L.; Hirsch, L. R.; West, J. L.; Halas, N. J. *Appl. Phys. Lett.* **2003**, *82*, 257. (b) Jackson, J. B.; Halas, N. J. *Proc. Natl. Acad. Sci. U.S.A.* **2004**, *101*, 17930−17935.

(8) (a) Krug, J. T.; Wang, G. D.; Emory, S. R.; Nie, S. *J. Am. Chem. Soc*. **1999**, *121*, 9208. (b) Emery, S. R.; Haskins, W. E.; Nie, S. *J. Am. Chem. Soc.* **1998**, *120*, 8009. (c) Lyon, W. A.; Nie, S. *Anal. Chem.* **1997**, *69*, 3400. (d) Nie, S.; Emery, S. R. *Science* **1997**, *275*, 1102. (e) Doering, W. E.; Nie, S. *J. Phys Chem B* **2002**, *106*, 311−317. (f) Kneipp, K.; Wang, Y.; Kneipp, H.; Itzkan, I.; Dasari, R. R.; Feld, M. S. *Phys. Rev. Lett*. **1996**, *76*, 2444. (g) Kneipp, K.; Kneipp, H.; Itzkan, I.; Dasari, R. R.; Feld, M. S. *Chem. Phys.* **1999**, *247*, 155. (h) Bjerneld, E. J.; Foldes-Papp, Z.; Käll, M.; Rigler, R. *J. Phys. Chem. B* **2002**, *106*, 1213−1218. (i) Xu, H.; Bjerneld, E. J.; Käll, M.; Borjesson, L. *Phys. Rev. Lett*. **1999**, *83*, 4357−4360. (j) Michaels, A. M.; Jiang, J.; Brus, L. *J. Phys. Chem. B* **2000**, *104*, 11965. (k) Bosnick, K. A.; Jiang, J.; Brus, L. E. *J. Phys. Chem. B* **2002**, *106*, 8096.

(9) Moskovits, M.; Tay, L.; Yang, J.; Haslett, T. *Top. Appl. Phys*. **2002**, *82*, 215−226.

(10) Aravind, P. K.; Metiu, H. *Surf. Sci.* **1983**, *124*, 506−528.

(11) (a) Mirkin, C. A.; Letsinger, R. L.; Mucic, R. C.; Storhoff, J. J. *Nature* **1996**, *382*, 607−609. (b) Mucic, R. C.; Storhoff, J. J.; Mirkin, C. A.; Letsinger, R. L. *J. Am. Chem. Soc.* **1998**, *120*, 12674−12675.

(12) Vlčková, B.; Matějka, P.; Šimonová, J.; Pančoška, P.; Čermáková, K.; Baumruk, V. *J. Phys. Chem*. **1993**, *97*, 9719.

(13) Sandhyarani, N.; Pradeep, T. *Vacuum* **1998**, *49*, 279−284.

(14) Bensebaa et al. *Spectrochim. Acta, Part A* **1999**, *55*, 1229−1236.

(15) (a) Tuinstra, F.; Koenig, J. L. *J. Chem. Phys*. **1970**, *53*, 1126. (b) Yoshizawa, K.; Okahara, K.; Sato, T.; Tanaka, K.; Yamabe, T. *Carbon* **1994**, *32*, 1517. (c) Castiglioni, C.; Mapelli, C.; Negri, F.; Zerbi, G. *J. Chem. Phys*. **2001**, *114*, 963. (d) Livneh, T.; Haslett, T. L.; Moskovits, M. *Phys. Rev. B: Condens. Matter Mater. Phys.* **2002**, *66*, 195110.